# Plug-in cross-dispersing module for the Large Binocular Telescope's infrared spectrograph LUCI

**Hyukmo Kang**[a], **David Thompson**[b], **Al Conrad**[b], **James Wiese**[b], **Heejoo Choi**[a,b], **Vishnu Reddy**[c] and **Daewook Kim**[a,b,d,*]

[a]University of Arizona, James C. Wyant College of Optical Sciences, Tucson, Arizona, United States

[b]Large Binocular Telescope Observatory, Tucson, Arizona, United States

[c]University of Arizona, Lunar and Planetary Laboratory, Tucson, Arizona, United States

[d]University of Arizona, Department of Astronomy, Tucson, Arizona, United States

**Abstract.** The large binocular telescope (LBT) can spectrally characterize faint objects from the ultraviolet (UV) to the near infrared (NIR) using two instruments, such as multiobjects double spectrograph (MODS) and LBT utility camera in the infrared (LUCI), which are pairs of imagers and spectrographs. Although LUCI can cover the NIR bands (0.9 to 2.4 $\mu$m), we currently need to use both LUCIs at the same time with existing gratings and filters. We report on the design and initial construction of a modular system called mask-oriented breadboard implementation for unscrambling spectra (MOBIUS) that enables a single LUCI to produce a full NIR spectrum (0.9 to 2.4 $\mu$m) in a single exposure. MOBIUS is a Littrow type spectrograph that is installed within the limited space of exchangeable mask frame space of LUCI. This plug-in concept requires no modification to the current instrument while dispersing the input slit perpendicular to the dispersion direction of the gratings in LUCI. With MOBIUS, we can utilize a slit length up to 2.3 arcsecond to acquire zJHK spectra without mixing orders at the LUCI image plane. In binocular observations with the LBT, a MODS spectrograph will be used with a LUCI + MOBIUS to acquire spectra across the full optical NIR wavelength range from 0.3 to 2.4 $\mu$m simultaneously. This will benefit studies of transient sources from rotating asteroids in our solar system to gamma-ray bursts, as well as anything with broad spectral features or unknown redshifts. The design process, tolerances, and initial table-top testing results to verify the operation of MOBIUS are presented in this work.  [DOI: 10.1117/1.JATIS.8.4.045003]

**Keywords:** Large Binocular Telescope; Large Binocular Telescope utility camera in the infrared; infrared; spectrograph; cross dispersion; instrument design.

Paper 22042G received Mar. 30, 2022; accepted for publication Nov. 14, 2022; published online Dec. 2, 2022.

## 1 Introduction

Spectroscopy can provide information about the surface chemical composition as well as physical state of the target being studied. For instance, asteroids are commonly composed of materials ranging from pyroxene and olivine to metallic nickel-iron. Ultraviolet to near-infrared (NIR) spectra (0.3 to 2.5 $\mu$m) have been widely used to determine surface compositions of asteroids[1] as they have diagnostic spectral features in these bands. While suitable spectra covering the UV-optical NIR can be obtained from various telescopes and instruments, there are distinct advantages coming from obtaining the data simultaneously. Because asteroids rotate, simultaneous spectroscopy allows all data to be associated with the same surface features. Simultaneous data obtained from the same telescope will be largely free from site-specific variability issues, such as seeing and nonphotometric weather. A broad wavelength coverage increases the chances of getting more spectral features and allowing an unambiguous identification for rapidly variable objects, such as gamma ray bursts.

*Address all correspondence to Daewook Kim, dkim@optics.arizona.edu

2329-4124/2022/$28.00 

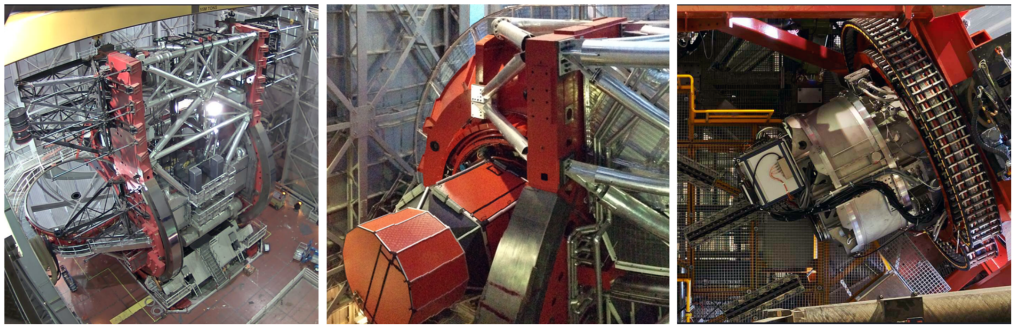

(a) (b) (c)

**Fig. 1** Photos of (a) LBT, (b) one unit of MODS, and (c) one unit of LUCI. Both MODS and LUCI are installed on both sides of the binocular telescope. Therefore each side could be configured with different instruments (mixed-mode), such as LUCI and MODS.[2]

The Large Binocular Telescope (LBT) consists of two 8.4 m diameter f/15 Gregorian telescopes on a common mount [Fig. 1(a)].[3] Two pairs of facility instruments can spectrally characterize faint objects from UV to NIR wavelengths: [the multiobjects double spectrographs (MODS), covering 0.32 to 1 $\mu$m)] [Fig. 1(b)][2] and [LBT utility camera in the infrared (LUCI), covering 0.9 to 2.4 $\mu$m)] [Fig. 1(c)].[4] Each side of the LBT can be configured independently for depth using two identically configured MODS on the same target for example or for speed using multiobject masks covering two sets of targets in the same field.[5] We can also extend the wavelengths covered by running one MODS and one LUCI, but this currently works only out to $J$ band with the existing capabilities of LUCI. With new gratings being installed into LUCI for use with adaptive optics, we realized that a different configuration of the instrument could cover all four NIR bands (i.e., zJHK bands) in one exposure if we could achieve a cross-dispersion.

In this paper, we present our design of a cross-dispersing module called mask-oriented breadboard implementation for unscrambling spectra (MOBIUS), which produces a simultaneous zJHK spectrum with a single LUCI.[6] By combining this system with MODS through binocular observations, MOBIUS in LUCI extends simultaneous coverage from 0.32 to 2.40 $\mu$m with little penalty.[5] There were several requirements on MOBIUS that strongly impacted the final design discussed below.

## 2 Design of MOBIUS

### 2.1 *Concepts*

One of the primary requirements for MOBIUS is that no modifications to the existing LUCI instruments are allowed. With the camera and grating wheels fully populated, the only options were to insert a new filter or make use of the focal plane slit mask exchange mechanism that is used to move custom multiobject spectroscopic (MOS) masks or long slits into the telescope focal plane. This cryogenic robot is known as the MOS unit.[7] Because the filters sit near the detector in a relatively fast converging beam while the masks sit in the f/15 focal plane from the telescope, the MOS mask was the only viable location for MOBIUS. Use of the focal plane mask for MOBIUS imposes quite severe space constraints, as the available volume is only 150 mm $\times$ 150 mm $\times$ 12 mm. The MOS robot is also not infinitely strong, so we adopted a constraint of not exceeding the weight of a normal LUCI MOS mask + frame (about 306 g) by $>$ 20 g at the recommendation of the team that built LUCI.[8] Thus, if the space and weight constraints can be satisfied, we have a cross-dispersing unit easily deployed on demand (Fig. 2).

MOBIUS is also required to minimize the impact on the image quality at the LUCI detector plane while providing cross-dispersion in LUCI. This indicates that the optical properties of the incident beam from LBT (i.e., $f$-number, chief ray angle, and focal plane position) should be kept after the MOBIUS module is inserted. To verify the image quality, we compared the ensquared energy and spot diagram in each band for the LUCI-only case and with MOBIUS

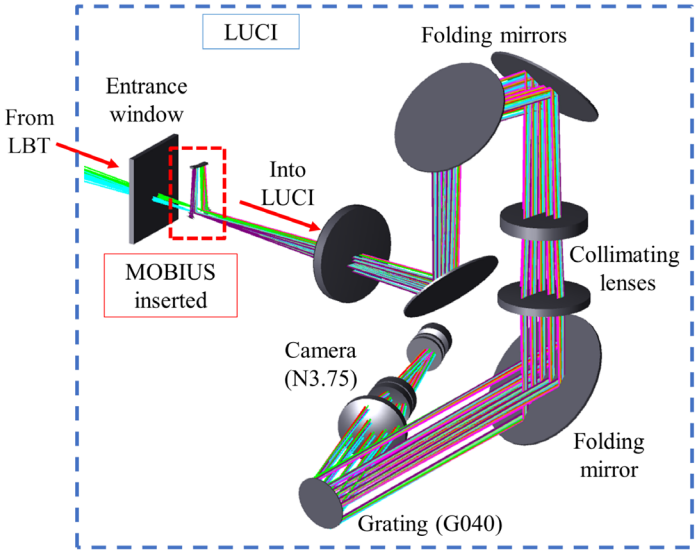


**Fig. 2** The optical layout shows how MOBIUS works with LUCI. The MOBIUS-installed frame will be placed at the focal plane of LBT by substituting the traditional slit mask frame. With MOBIUS, LUCI is able to observe zJHK spectra in a single exposure without mixing between wavelength bands without additional modification in instrument settings.

inserted. A table-top experiment with fabricated optical components was also performed to demonstrate the performance of MOBIUS. Finally, to deal with normal atmospheric variability in the NIR and maximize time on target, MOBIUS consists of two identical cross-dispersing modules symmetrically side by side in a single mask frame to offer sky subtraction by dithering between source and sky positions. They are mirrored rather than duplicated to minimize the effective separation on sky between the two entrance slits.

Littrow type spectrographs[9,10] fit perfectly to our concepts. With a mirror-coated rear surface, Littrow prism configurations utilize a double pass that enables increased dispersion in a compact form and returns dispersed rays to near the original slit position.

The schematic concept of MOBIUS is shown in Fig. 3.[6] The triangle shaped pick-off mirror is located at the focal plane of the LBT to deflect the incident beam toward into the space in the mask frame, and a slit will be installed right after the pick-off mirror [Fig. 3(a)]. The beam is then collimated with a spherical mirror and enters the Littrow prism, which provides both dispersion and retro-reflection. After reflection, the dispersed beam hits the spherical mirror again and is reimaged on the other side of the pick-off mirror where it is reflected into LUCI [Fig. 3(b)]. Because the dispersed beams are still within the field of view of LUCI, there would be no vignetting as long as the ray angle and focal planes have remained unchanged from the original LBT beam. As the beam is dispersed at the focal plane of LBT to the perpendicular direction of LUCI's dispersion, MOBIUS separates the multiple orders delivered by LUCI's grating to broaden the wavelength coverage of a single LUCI with no modification to the instrument.

## 2.2 *Optical Design Process*

As a goal for producing scientifically useful data, MOBIUS should provide a large enough dispersion distance to prevent overlapping between diffraction order spectra at the LUCI detector while securing the minimum slit length, 2 arcsecond, corresponding to 1.2 mm of dispersion distance. Allowing a small margin between spectral orders at the detector, we set our target minimum dispersion distance between the central wavelengths of each order as 1.5 mm at the exit surface of pick-off mirror.

MOBIUS consists of three optical components: a pick-off mirror, a spherical mirror as collimator, and a Littrow dispersing prism, which has a mirror-coated rear surface. The specific parameters of each component are determined considering dispersion distance, maximum beam footprint size, and the best focal region of the LBT. The shape of the pick-off mirror

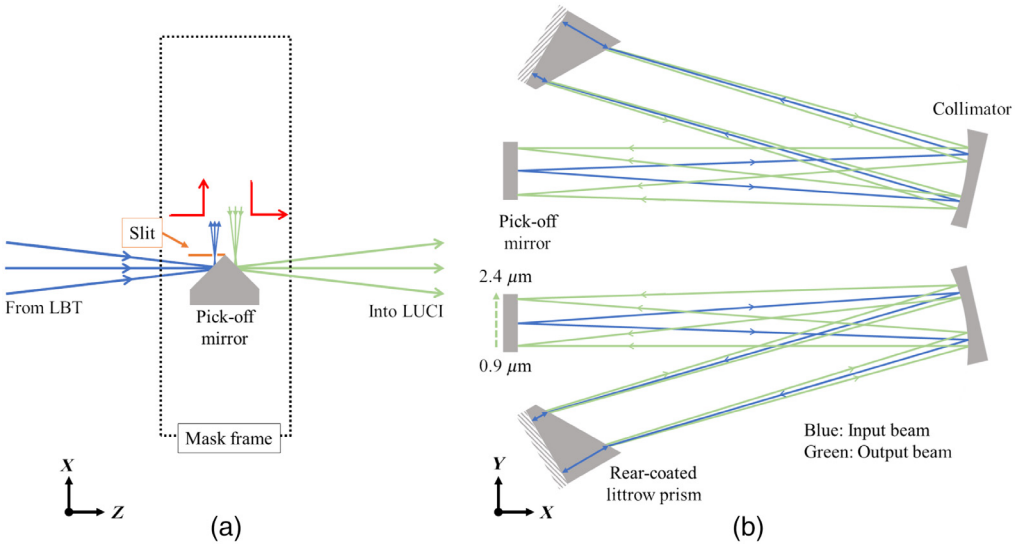


**Fig. 3** Schematic figure of MOBIUS.[6] (a) View inplane of slit mask: the pick-off mirror is placed near the focal plane of the LBT to deflect the input beam path (blue lines) into the plane of the mask frame. The return beam from MOBIUS is reflected into LUCI on the other surface of the pick-off mirror (green lines). (b) View seen from sky: inside of the frame mask, the beam from the telescope (blue) is collimated, dispersed, and then reimaged (green lines) back to the pick-off mirror. This process produces the cross-dispersion before the higher dispersion grating in LUCI. MOBIUS consists of two identical spectrographs to offer sky subtraction by dithering between target and sky position.

is a right-angle prism, yet the outer surfaces are employed for reflection [Fig. 4(a)]. Because the dispersed beam is retroreflected, the input and output beams are nearly parallel to each other. So the apex angle of the pick-off mirror is designed to be 90 deg to preserve the ray angles before and after MOBIUS. The location of the pick-off mirror inside the slit mask frame was kept near the center of the mask as it is determined by the best focal region of the LBT ($\pm 1.25$ arcminute in dispersion direction of LUCI, which is perpendicular to the dispersion direction of MOBIUS)[7] as well as the focal length of the collimating mirror.

For the collimating mirror [Fig. 4(b)], although an off-axis parabolic mirror is commonly used, we chose a spherical mirror because it made negligible aberration on the slow f/15 beam from the telescope. The spherical mirror has advantages in fabrication and alignment as well. The focal length of a spherical mirror is directly related to the dispersion distance because the longer focal length produces greater dispersion. We set the radius of curvature of the spherical mirror to 180 mm in MOBIUS. As a consequence, we could secure some margin at the clear aperture of spherical mirror while extending slit length for scientific objectives.

The Littrow dispersing prism [Fig. 4(c)] is made of strontium titanate ($SrTiO_3$, $n = 2.28$ at $\lambda = 1.65$ $\mu$m), which is transmissive and highly dispersive at the operating wavelengths and

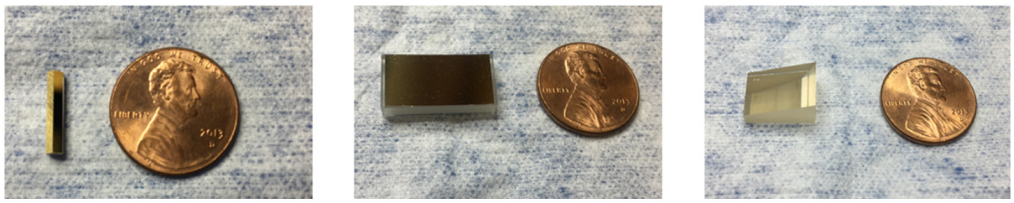


**Fig. 4** Fabricated optical components of MOBIUS.[11] (a) The pick-off mirror is made of Zerodur and is gold coated. The clear aperture is 12 mm by 2 mm. (b) The spherical mirror is made of Zerodur and aluminum-coated. Clear aperture is 17.5 mm by 9 mm. (c) Littrow prism with silver-coated on rear surface. The entrance surface has about 13 mm by 8 mm of clear aperture.

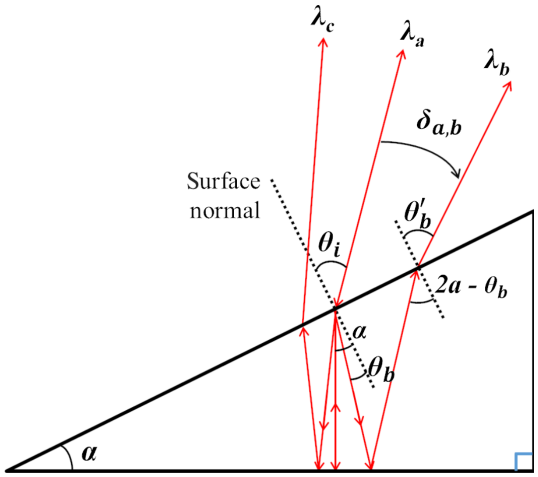


**Fig. 5** Ray diagram of Littrow prism. The apex angle ($\alpha$) of prism should be equal to the refractive angle to make retroreflection.

temperature.[12,13] The apex angle of the prism determines dispersion distance. To calculate the dispersion distance between two wavelengths, we need to find the deviation angle difference first. In the Littrow prism (Fig. 5), the apex angle ($\alpha$) is equal to the refractive angle to make the refractive ray is reflected as normal to the rear surface. So, the incident angle $\theta_i$ is determined as

$$\theta_i = \sin^{-1}(n_a \sin \alpha), \tag{1}$$

where $n_a$ is refractive index of wavelength $\lambda_a$. Assumed that the base wavelength is $\lambda_a$, the refracted angle ($\theta_b$) of wavelength $\lambda_b$ inside of prism is

$$\theta_b = \sin^{-1}\left(\frac{n_a}{n_b}\sin \alpha\right). \tag{2}$$

Now, the beam is reflected from the rear surface, and resulted refracted angle from the prism ($\theta'_b$) is

$$\theta'_b = \sin^{-1}[n_b \sin(2\alpha - \theta_b)]. \tag{3}$$

Thus, deviation of $\lambda_b$ when the base wavelength is $\lambda_a$ ($\delta_{a,b}$) is

$$\delta_{a,b} = \theta'_b - \theta_i \quad = \theta'_b - \sin^{-1}(n_a \sin \alpha). \tag{4}$$

Therefore the dispersion distance ($\Delta d_{a,b}$) is

$$\Delta d_{a,b} = f \tan(\delta_{a,b}), \tag{5}$$

where $f$ represents the focal length of the spherical mirror.

MOBIUS is required to separate the four NIR bands corresponding to the orders of G040 grating in LUCI. The blaze wavelength of each band is 0.96 ($z$), 1.2 ($J$), 1.6 ($H$), and 2.4 $\mu$m ($K$).[14] We found the apex angle of prism to make minimum dispersion requirement between $J$ band and $H$ band because the refractive indices of $SrTiO_3$ shows the lowest difference there. This condition and Eq. (5) lead to an apex angle of 19 deg. Also, the incident angle for retroreflection is 48 deg and the dispersion distance between the $J$ and $H$ band is 1.65 mm at the focal plane of the LBT, which meets our requirement.

The optical design of a unit of MOBIUS is shown in Fig. 6(a),[6] and the overall layout with optical components mounted in a slit mask frame is in Fig. 6(b). The light-weighted features are implemented on the frame to meet the safe weight requirement (total frame weight of 326 g) of the MOS unit. We also added alignment screws in the MOBIUS module for fine adjustment.

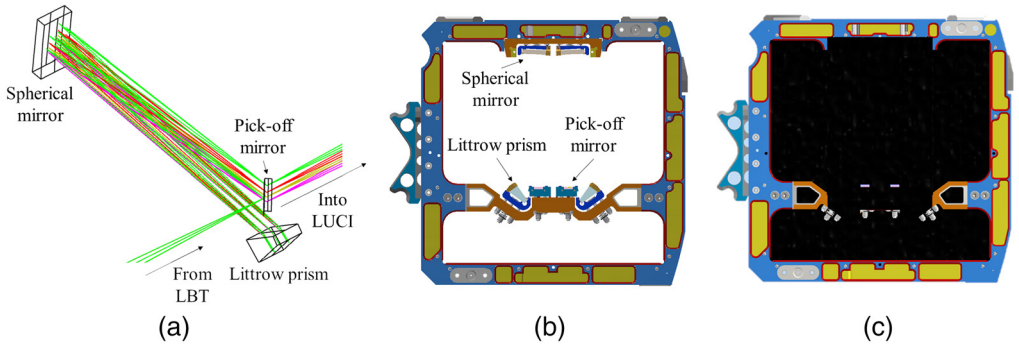


**Fig. 6** (a) Optical layouts of a unit of MOBIUS.[6] (b) The layout of MOBIUS mounted slit mask frame with alignment features. We light-weighted the frame to meet the weight limit of MOBIUS. Two identical spectrographs are located in plane symmetry, and the slits are placed as close as possible for the sky subtraction by dithering. (c) MOBIUS with mask (black color). The mask blocks empty space of frame except the entrance to MOBIUS.

**Table 1** Tolerance results for alignment of each component and apex angle of the pick-off mirror.

| | Dx (mm) | Dy (mm) | Dz (mm) | Tx (mrad) | Ty (mrad) | Tz (mrad) |
|---|---|---|---|---|---|---|
| Pick-off mirror | — | — | — | 1.4 | 1.7 | — |
| Spherical mirror | 0.2 | 0.2 | 0.3 | — | 1.4 | 1.13 |
| Prism | 0.5 | 0.5 | 0.5 | — | 1.7 | 1.7 |
| Apex angle of pick-off mirror | | | 89.87 deg $\leq \alpha \leq$ 90.04 deg | | | |

The main concern for MOBIUS is vignetting as the optical performance remains good enough as long as the beam is not vignetted. We performed a sensitivity analysis to figure out the alignment tolerance of each optical component. $Z$-axis is defined along with beam path of LBT, and $Y$-axis is the direction of dispersion from MOBIUS. Table 1 shows the tolerance results for MOBIUS. Translation in $x$, $y$, and $z$-axis are denoted as Dx, Dy, and Dz for each and tilt about $x$, $y$, and $z$-axis are denoted as Tx, Ty, and Tz. As the entrance slit is coupled together, the X, Y, and Z coordinate of the pick-off mirror is set as reference. Tolerances of Tz of pick-off mirror, Tx of spherical mirror, and prism are not specified as they have minor effects only. Overall alignment tolerance is quite generous while the apex angle of the pick-off mirror is the most sensitive factor for vignetting. The tolerable range of apex angle of the pick-off mirror ($\alpha$) is from −2.27 to 0.7 mrad from the designed value 90 deg.

The MOBIUS-installed mask frame itself is insensitive to the alignment. This is because (1) the pick-off mirror has 90 deg of apex angle, and (2) the spherical mirror and dispersion prism will work as a retro reflector so that MOBIUS will keep the ray angle from LBT.

## 3 Performance Analysis

### 3.1 *Designed Performance*

The footprint diagram for LUCI without and with MOBIUS are shown in Fig. 7.[6] In LUCI alone, [Fig. 7(a)], all the spectra are overlapped in a line so that the use of an order-sorting filter is essential to separate the different bands. In contrast, as MOBIUS generates perpendicular dispersion to LUCI, each of the four orders are separated and distinguishable [Fig. 7(b)]. In the current design, MOBIUS can utilize a slit length up to 2.3 arcsecond without mixing different wavelength bands.

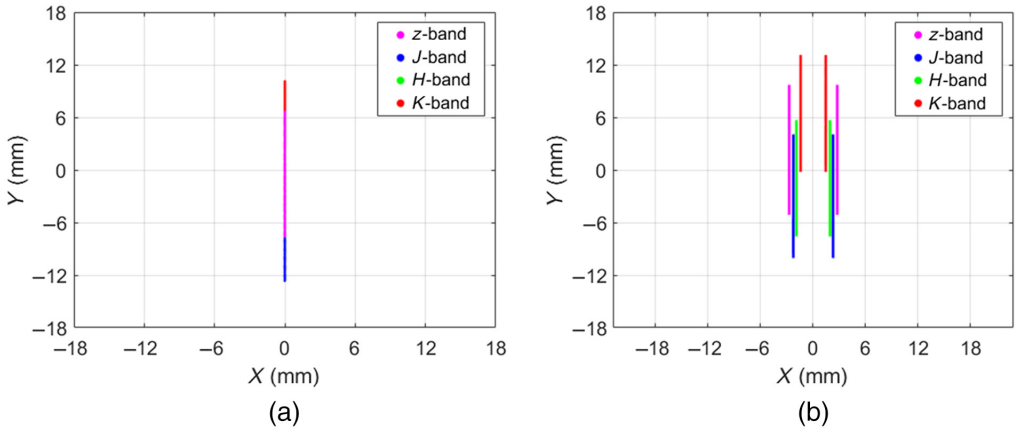


**Fig. 7** Spectroscopic results at the LUCI detector. When observing using (a) LUCI alone and (b) LUCI with MOBIUS. With MOBIUS, spectra of each order are not overlapped up to 2.3 arcsecond of slit length. The range of each spectrum is determined by the usable wavelength limits by G040 grating.[14] Two sets of zJHK spectra represents the two spectrographs in the MOBIUS which are mirror-symmetric. The symmetric configuration allows the entrance slits to be closer to each other on sky.[6]

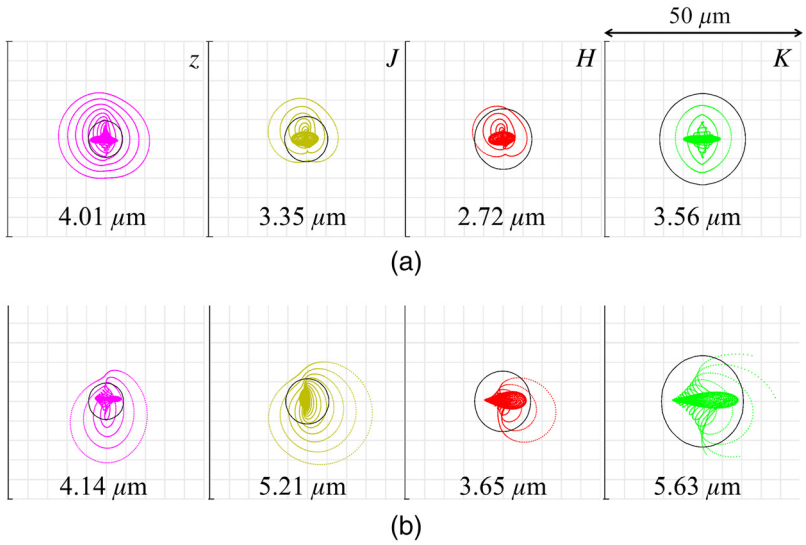


**Fig. 8** Spot diagrams at the N3.75 camera detector plane of (a) LUCI and (b) LUCI with MOBIUS in each wavelength band. Numbers in the figure show the rms radius of each spot diagram, and the black circles at the center represent Airy disk size of blaze wavelength of each band. Although the rms value is increased after the MOBIUS, the rms radius is increased less than a detector pixel size (18 $\mu$m) from each spot diagram.

In addition to the cross-dispersion MOBIUS provides, another important requirement is that MOBIUS maintains the image quality of LUCI while it is in the beam. We compared the spot diagrams (Fig. 8) and ensquared energy at the LUCI detector plane (Fig. 9)[6] to verify that the image quality remains the same with MOBIUS. Although the overall radius of the rms spot size has slightly increased with MOBIUS in the beam (Fig. 8), they are still similar to the Airy disk size, and the difference is less than a detector pixel size (18 $\mu$m). In the ensquared energy case (Fig. 9), the most measurable difference is at $K$ band in half width distance for 90% fraction energy, which is $\sim$2 $\mu$m. Because the expected seeing disk size delivered by the telescope is $>$2 pixels on the N3.75 camera, we can assume that MOBIUS is not a limiting factor in the image quality while expanding wavelength coverage of LUCI with little penalty.

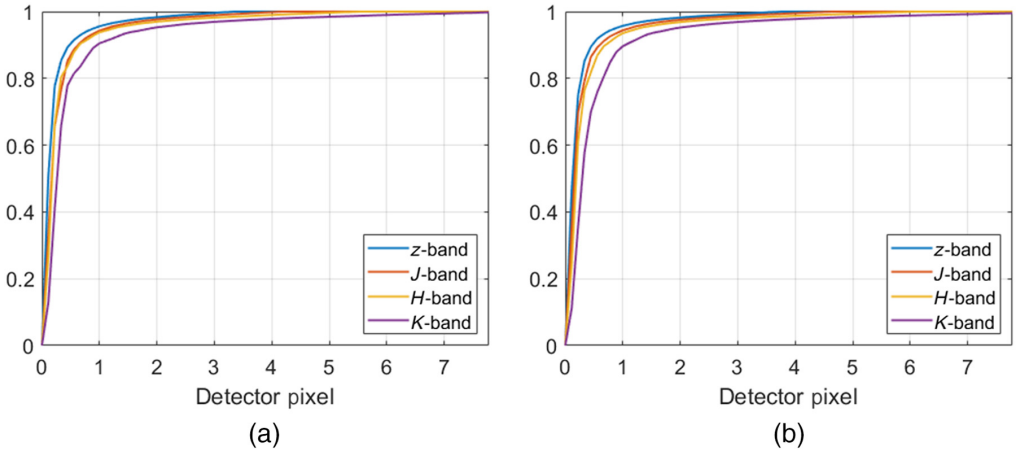


**Fig. 9** Ensquared energy comparison between (a) LUCI and (b) LUCI with MOBIUS-equipped. In every wavelength band, the difference in half width distance between LUCI and MOBIUS for 90% fraction energy is less than a pixel of the detector. This difference is insignificant as the expected seeing disk size is >2 pixels or 0.25 arcsecond.[6]

## 3.2 *Table-top Result*

The table-top test was performed with the optical components assembled in a rigid aluminum frame [Fig. 10(a)]. We used a xenon light bulb as a light source to secure broad NIR wavelength (from 0.9 to 1.7 $\mu$m) and formed an f/15 beam to simulate the LBT [Fig. 10(b)]. The specification of the detector we used[15] is summarized in Table 2.

The table-top results are shown in Fig. 11. The length of resulting MOBIUS-dispersed spectrum is about 110 pixels (3.3 mm) at the detector. Considering the quantum efficiency of the detector, this result is validated with the expected spectrum length from the Zemax model (3.6 mm).

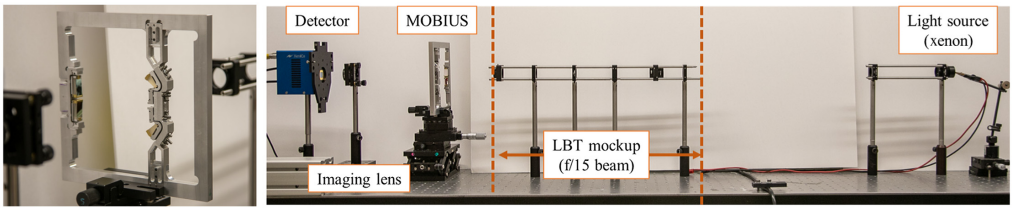


**Fig. 10** (a) MOBIUS with rigid aluminum frame is mounted in the table-top test setup. This frame allows alignment and testing of the MOBIUS optics in their proper positions. (b) The test setup of MOBIUS.

**Table 2** Specification of detector.[15]

| | XEVA-FPA-320 by XenICs |
|---|---|
| Type | InGaAs |
| Format | 320 × 256 pixels |
| Pixel pitch | 30 $\mu$m |
| Spectral range | 900 to 1700 $\mu$m |

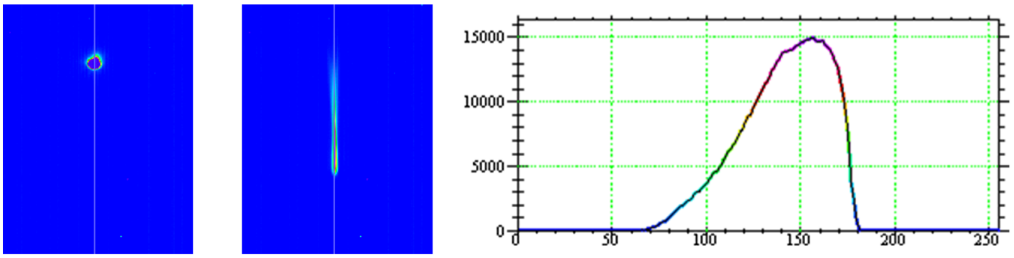


**Fig. 11** The table-top results: (a) image without MOBIUS and (b) with MOBIUS. (c) The profile of MOBIUS spectrum along with the center gray line in panel (b). The length of the MOBIUS spectrum is about 110 pixels (3.3 mm), which corresponds to the expected result from the Zemax model (3.6 mm).

## 4 Conclusion

In this paper, we presented MOBIUS, a cross-dispersion module that expands wavelength coverage of the existing NIR spectroscopic instrument (i.e., LUCI). As MOBIUS is installed in a slit mask frame and utilizes current control hardware (i.e., the MOS unit), additional modification to the current instrument is not necessary. With a Littrow prism configuration, MOBIUS provides simultaneous and continuous spectrum from 0.86 to 2.4 $\mu$m for a single LUCI unit while having minimal impact on ensquared energy. A table-top test was performed to validate the performance of MOBIUS. With MOBIUS, LUCI can cover the four NIR bands simultaneously with up to 2.3 arcsecond of slit length. An instrument with the capabilities of MOBIUS would be useful for studies of asteroids and other faint objects in the solar system via the mixed operating mode of LBT, such as one MODS and one MOBIUS-equipped LUCI to observe a target simultaneously from UV to NIR wavelengths.

## Acknowledgments

The LBT is an international collaboration among institutions in the United States, Italy and Germany. LBT Corporation Members are: The University of Arizona on behalf of the Arizona Board of Regents; Istituto Nazionale di Astrofisica, Italy; LBT Beteiligungsgesellschaft, Germany, representing the Max-Planck Society, The Leibniz Institute for Astrophysics Potsdam, and Heidelberg University; The Ohio State University, representing OSU, University of Notre Dame, University of Minnesota, and University of Virginia. Parts of this research were supported by the State of Arizona Technology Research Initiative Fund (TRIF) through the Space4 Center at the University of Arizona.

## References

1. V. Reddy et al., "Mineralogy and surface composition of asteroids," in *Asteroids IV*, P. Michel et al., Eds., pp. 43–63, University of Arizona, Tucson, Arizona (2015).
2. R. W. Pogge et al., "The multi-object double spectrographs for the large binocular telescope," *Proc. SPIE* **7735**, 77350A (2010).
3. J. M. Hill et al., "The large binocular telescope: binocular all the time," *Proc. SPIE* **9145**, 914502 (2014).
4. H. Mandel et al., "LUCIFER status report: summer 2008," *Proc. SPIE* **7014**, 70143S (2008).
5. B. Rothberg et al., "Current status of the facility instruments at the Large Binocular telescope Observatory," *Proc. SPIE* **10702**, 1070205 (2018).
6. H. Kang et al., "Modular plug-in extension enabling cross-dispersed spectroscopy for large binocular telescope," *Proc. SPIE* **11116**, 1111606 (2019).
7. P. Buschkamp et al., "The LUCIFER MOS: a full cryogenic mask handling unit for a near-infrared multi-object spectrograph," *Proc. SPIE* **7735**, 773579 (2010).

8. R. Hofmann et al., "The cryogenic MOS unit for LUCIFER," *Proc. SPIE* **5492**, 1243–1253 (2004).
9. I. Ilev, "Simple autocollimation laser refractometer with highly sensitive, fiber-optic output," *Appl. Opt.* **34**(10), 1741–1743 (1995).
10. D. W. Warren and S. Lampen, "Littrow spectrographs for moderate resolution infrared applications," *Proc. SPIE* **9976**, 18–23 (2016).
11. D. Kim et al., "Advances in optical engineering for future telescopes," *Opto-Electron. Adv.* **4**(6), 210040–210040 (2021).
12. M. Bass and Optical Society of America, *Handbook of Optics*, 2nd ed., McGraw-Hill, New York (1995).
13. J.-F. Lavigne, "Design of an infrared integral field spectrograph specialized for direct imaging of exoplanets," *Proc. SPIE* **6342**, 63421M (2006).
14. J. Heidt and D. Thompson, "LUCI user manual," (September 7, 2016). https://sites.google.com/a/lbto.org/luci/documents-and-links
15. I. Foppiani et al., "An infrared test camera for LBT adaptive optics commissioning," *Proc. SPIE* **7015**, 701562 (2008).

**Hyukmo Kang** is working as a postdoctoral researcher at the James C. Wyant College of Optical Science of the University of Arizona. He is also serving as an instructor of practical optical system design workshop at the University of Arizona. His research interests include optical design, fabrication, and metrology for astronomical and industrial applications.

**David Thompson** is working as an astronomer at the LBT, primarily on instrumentation support for the two LUCI infrared imaging spectrographs. He was also involved in the early telescope and instrument focal station commissioning at the LBT. His research interests include developing novel instrumentation, such as MOBIUS, as well as optimizing observation and data reduction techniques.

**Heejoo Choi** is working as an assistant research professor at the James C. Wyant College of Optical Science of the University of Arizona. He contributed to designing, modeling, and testing multiple space projects. He is also working at Large Binocular Telescope as an optical scientist and developing collimation and pointing methodology. He has been serving the optics community as an editor for journals and conference chair. His research interests include optical design and metrology for academia and industrial systems.

**Daewook Kim** is working as a faculty of optical sciences and astronomy at the University of Arizona. He has been working on various optical engineering projects, including NASA Aspera UV space telescope mission, 25-m diameter Giant Magellan Telescope, and commercial augmented reality freeform glass projects. He has been chairing international conference programs, including Optica and SPIE conferences. He has published more than 200 journal/conference papers. He gave more than 20 plenary, keynote, and colloquium talks.

Biographies of the other authors are not available.